ChemPhysChem

Chemistry Europe
European Chemical Societies Publishing

Reprint

WILEY-VCH

Surface Propensity of Anions in a Binary Ionic-Liquid Mixture Assessed by Full-Range Angle-Resolved X-ray Photoelectron Spectroscopy and Surface-Tension Measurements

Erdinc Oz,[a] Ozgur Sahin,[a] Halil I. Okur,[a] and Sefik Suzer*[a]

Angle-resolved X-ray photoelectron spectroscopy and contact-angle measurements guided by a signal attenuation model are utilized to extract molar composition and anion enrichment in the vacuum interface of a binary ionic liquid mixture, having a common quaternary ammonium cation and two different anions. By using the intensity ratio of the F1s peaks belonging to the two different anions recorded at the full electron take-off angle range, from 0° to 80°, we have determined that only a fractionally covered and anion enriched surface layer can predict the AR-XPS data, which is also consistent with surface tension measurements. Moreover, the more bulky and non-spherical anion enrichment is evident even at the conventional and the so assumed bulk sensitive take-off angle of 0°. This methodology provides a surface enrichment factor of the molecular ions and clearly serves as an experimental evidence for recently debated surface layering and/or island structure in ionic liquid systems.

Ionic liquids (IL) and their mixtures have recently gained traction in many fields including, but not limited to, pharmaceuticals and battery electrolytes.[1] This newfound interest is mainly due to their convenient chemical/physical properties such as, extremely low volatility, adequate conductivity and malleability of their properties for different applications.[2] The IL mixtures in particular, have piqued the interest of many researchers because of their ease of manufacturing relative to synthesizing new ionic liquids for fine-tuning their properties. The mixtures are also convenient for the fact that some show almost ideal behavior which makes it easier to predict their bulk properties.[3–5] However, while their bulk properties enjoy this predictability, surface composition and properties of most ILs and their mixture, which are important for applications such as gas storage, catalytic activity and nanoparticles synthesis, are currently not well delineated.[6]

Existent studies on surface investigations of neat ILs utilize a multitude of techniques such as: Atomic Force Microscopy,[7] Sum-Frequency Generation,[8] Small-Angle X-Ray and Neutron Scattering,[9] High-Resolution Rutherford Backscattering Spectroscopy (HRBS) and Time-of-Flight Secondary Ion Mass Spectrometry (ToF-SIMS),[10] Low-Energy Ion Scattering (LEIS),[11] and Angle-Resolved-X-ray Photoelectron Spectroscopy (AR-XPS).[12] The novel experimental findings that emerged from these studies, have also successfully been corroborated and/or guided by extensive molecular dynamics (MD) simulations.[5c,9b,10b,13a,b]

Attempts at elucidating the surface composition of ILs and their mixtures have generally found that surfaces favor one or more of the constituents. For ILs containing long hydrocarbon chains such as 1,3-dialkylimidazolium group cations, it has been found that they act like surfactants, where the long alkyl groups are favored in the surface region facing away from the liquid while the imidazolium moiety is favored facing towards the liquid.[10b,12b] Moreover, a deeper, but somewhat conflicting understanding at the nano- and/or meso-level structuring into polar and nonpolar domains of both bulk and surface moieties has evolved, as a result of colossal efforts of many researchers in the field, in assessing the intricate roles played by ions, hydrogen bonding and alkyl chains in neat ILs as well as in their mixtures, using a multitude of experimental and/or simulation techniques over the last one and a half decade.[1a,2,4b,7] Recent developments and future expectations on various aspects of the IL research have recently been reviewed and compiled as a dedicated thematic issue of the Chemical Reviews journal.[14] However, structure and physical/chemical nature of these so-called polar-nonpolar domains, bi-layers or islands are still active topics of discussions and disputes, leaving for plenty of room and calling for further improvements.[1a,2,15]

XPS, and AR-XPS in particular have been repeatedly shown to be an invaluable technique for probing the surface chemical make-up of ILs and their mixtures.[3a,4a,b,12a] The surface sensitivity up to 6–8 nm in XPS is pivotal in determining the elemental and chemical composition of the surfaces, while AR-XPS gives another layer of sensitivity for detecting which constituents are more abundant near the surface. As a general practice, AR-XPS has been employed to measure only at two angles, commonly 0° and 80°, experimentally to inspect the molar composition of the constituents. This is sufficient for obtaining an estimate of the cation-anion ratio at a specific point near the surface but not for acquiring a composition profile with respect to liquid depth.[4a,b,12a,16a,b,17]

In principle the methodology for linking a given concentration profile to angle dependent XPS signal(s) is straightforward, but the inverse process, i.e. extracting a depth profile

[a] Dr. E. Oz, O. Sahin, Dr. H. I. Okur, Prof. S. Suzer
Department of Chemistry, Bilkent University,
06800 Ankara, Turkey
E-mail: suzer@fen.bilkent.edu.tr

Supporting information for this article is available on the WWW under https://doi.org/10.1002/cphc.202000750

from a given set of angle resolved spectra, is not, and requires certain geometrical modeling.[18] Generally, other experimental and/or simulation techniques such as: Surface tension, surface sensitive scattering measurements, molecular dynamics simulations, etc. are needed for validating the XPS data. Recent works of Steinruck's and Newberg's groups can be given as examples of such successful applications.[13b,15c]

Herein, we will report angle-resolved XPS data using the full-range (0° to 80° with an increment of 10°) with geometrical modeling to assess its potential for extracting more detailed depth information about the anion distribution in mixtures of two ILs having a common cation ($DEME^+$) and two different anions ($TFSI^-$ and BF_4^-), chemical structures of which are given in Scheme S1 of the Supporting Information section (SI). The results are correlated with the contact angle measurements of the corresponding mixtures. These ILs and their mixtures have been chosen, because: (i) Both have fluorine atoms representing their anions, which allows accurate determination of their ratio using the F1s peaks with lab-based XPS instruments, (ii) have been well-interrogated by other techniques, and (iii) surface enrichment of one ion over the others is expected on account of a large surface tension difference ($\Delta\gamma$), approaching 20 mN/m.[10b] Although AR-XPS has been utilized extensively in IL research, surprisingly, exploration of the full potential of the technique has not been reported before.

A thermo Fisher K-alpha X-ray photoelectron spectrometer was used to collect all data for the XPS measurements. For angle-resolved measurements the tilt-stage was utilized for take-off angles ranging from 0° (with respect to the surface normal) to 80° with 10° steps. The liquid samples were introduced as thin films, covering an area of ~3×3 mm of a metallic substrate, where the liquid is protruding from a ~0.5 mm ditch. A Dataphysics OCA 15 Plus system was used for contact angle measurements and drop shape analysis of liquid drops placed onto a ~20 μm polypropylene (PP) sheet. ^{19}F-NMR and FTIR spectra of the two ionic liquids and their nominal 1:1 mixture are given in Figures S1 and S2 in the SI Section. The NMR spectrum, which is more reliable for ascertaining molar ratios in the bulk, yielded a ratio of 1.65±0.1, slightly higher than their expected ratio of 1.5. As such, we will use the ratios determined by NMR in all of our discussions and simulations (see also Table S1).

Both NMR and FTIR data indicate close to an ideal solution behavior in the bulk for all the mixtures analyzed, but surface properties are significantly altered, as exemplified by the contact angle measurements of different bulk compositions of IL depicted in Figure 1. Since the trends are on the focus, the cosine of the contact angle (cos (θ)), assumed to be proportional to the surface tension of the fluid on the hydrophobic PP surface, is plotted against the mole fraction, instead of the absolute surface tension.

In general, a multitude of chemical/physical parameters, related with both solid, liquid and especially their interfaces, contribute to the measured contact angles. However, the data presented in Figure 1(c) displays a gradual decreasing trend for the (cos (θ)) with increasing TFSI mole fractions. Such a gradual trend assures a negligible interfacial tension contribution arising

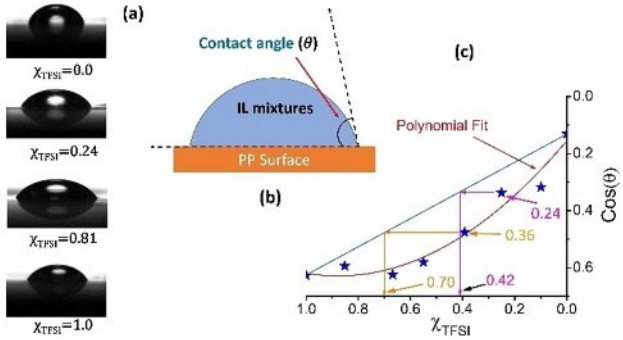

Figure 1. Contact angle measurements of the two pure liquids and their mixtures. **(a)** Recorded pictures of a few of the representative sessile drops on the PP substrate. **(b)** Schematics, and **(c)** Results of the Contact Angle Measurements.

from the direct IL and PP interactions based on Gibbs adsorption isotherm.[19]

Consistent with previous reports, starting from 0.10 mole fraction and on, a strong and close to a linear deviation from the ideal behavior sets in, and continues until about 0.67, indicative of the surface enrichment of the larger, more polarizable TFSI anion.[3a,5,10]

Conventional XP spectra reflect the stoichiometry of the liquids and their mixtures, once the atomic cross sections are taken into account, as shown in Figure 2 with a survey scan of a mixture having a mole fraction of 0.52. In the same figure, F1s region is also shown. Binding energy of the F1s in TFSI (i.e. $-CF_3$ groups) is higher than that in BF_4^-, therefore they appear as two well-separated peaks, similar to the cationic and anionic N1s peaks of the DEME-TFSI (see also Figure S3 in SI section). Since TFSI has two $-CF_3$ groups, for a 1:1 (DEME-TFSI:DEME-BF4) mixture F1s area ratio of the two peaks should be equal to 6:4. As also depicted in Figure 2(b) the F1s spectra recorded at two take-off angles for the same mixture reflects clearly ~20% depletion of the $BF4^-$ anion at the more surface sensitive observation angle of 60°. Moreover, the observed ratio at the

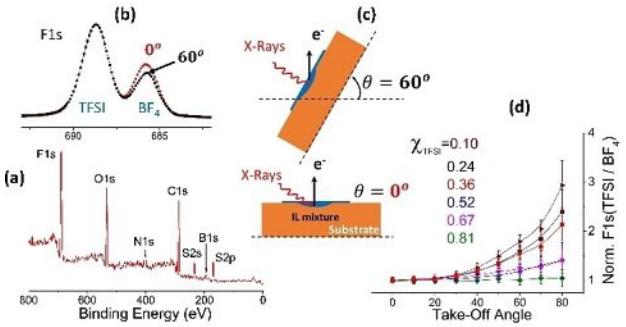

Figure 2. XP spectra of a nominal 1:1 IL mixture. **(a)** Survey and **(b)** F1s region at two different angles. **(c)** Schematics of the angle-resolved measurements. **(d)** Ratio of the two F1s peaks for different mixtures at different take-off angles normalized to that measured at 0°. Each data point was measured at least twice to ensure reproducibility.

more bulk sensitive take-off angle of 0° is 1.95 ± 0.1 (see also Figure S4 and Tables S1 and S2) also exhibiting measurable deviations from their expected values of 1.65, which is consistent with reports by Zhang,[15c] and Heller et al.[16a,b] for different IL mixtures. The surface sensitivity of the XPS technique, even at the normal photoemission angle, which is quite often considered to be bulk-sensitive, is further pronounced when also considering the fact that the NMR bulk ratio for this mixture is higher than the nominal value, but still significantly less than the XPS measurements.

Examination of Figure 2(d) reveals enrichments approaching to a factor of 3 at the grazing angle of 80°. Moreover, relative surface enrichment at the higher angles is inversely related with the mole fraction of TFSI, i.e. enrichment gets larger as dilution increases.

Information about the surface profile of the liquid mixtures could be extracted by analysis of the entire AR-XPS data, i.e. using more than just two angles, combined with a suitable geometrical model of the concentration profile of the two anions, and simulating intensity attenuation through the probed depth. In general, attenuation of XPS peak intensities as a function of the take-off angle is an exponentially decreasing function of the depth (**z**) from the surface and the take-off angle (■) or the detection angle with respect to the surface normal, due to the strong modulation of the ejected photoelectron passing through the sample. Similar to the Beer-Lambert absorption law, intensity attenuation is expressed as;

$$I_z = I_0{}^{*}\exp[-z/(\lambda^{*}\cos(\theta))] \quad (1)$$

where, **λ** is the attenuation length, I_0 and I_z are the intensities (peak areas) of the original signal, and the attenuated ones, respectively.[17] But, relative enrichment of anion or cation is expected to display an exponentially increasing trend with respect to the increasing take-off angle.[12a] From Figure 2(d) we see that the mixture with the TFSI mole fraction of 0.52 exhibits more than 40% enrichment at 80°, in total agreement with published AR-XPS data, and also with our contact angle measurements. But, we also gather from our experimental results that in none of the examined liquid mixtures, the F1s ratio of the two anions exhibits a clear exponential behavior, in contrast to what was reported by Lockett et al., for the C1s ratios of neat imidazolium ILs.[12a]

Several experimental parameters contribute to the outcome of AR-XPS data, some of which are sample specific, but there are also numerous other parameters that are instrument dependent. On the other hand, since we are comparing the same F1s core-level with resulting kinetic energies very close to each other, most of these parameters are expected to cancel out (e.g. photoemission cross-section of the analyte atom). Nevertheless, by using several relevant samples, we have carefully checked and validated our methodology, as outlined in detail in the (SI) Section, (see Figures S5, S6 and S7).

The simulation model we have adopted is a simple finite slab model with depth increments of 0.01 nm, representing the surface (z_S) as well as most of the bulk liquid (z_B) up to a depth of 20 nm. This value is more than sufficient considering the depth probed by XPS (3**λ** = ~9 nm), where the attenuation length is taken as 2.8 nm for the F1s peak.[20] Additionally, the number density of the TFSI in the surface (δ_S) and in the bulk (δ_B) layers are assumed to be different, as shown in Scheme 1. Accordingly, we define an enrichment factor (**EF**) as the ratio of the surface anion number density or the mole fraction to that in the bulk. For the 0.52 mixture, the bulk ratio is 1.65, hence any observed/simulated F1s intensity ratio divided by 1.65 and larger than 1, is referred as the enrichment factor. We also consider that such an enriched layer does not necessarily cover the entire surface of the mixture, hence possibility of fractional coverage is also included. Moreover, the fractionated surface layer does not have to be continuous, i.e. a patchy and random distribution would also give the same result, as indicated in the same scheme. Details of the procedure are given in the ***SI*** section. As outlined therein, we have tested several EFs and geometries with and without fractional coverage, in order to find the parameters to best match the AR-XPS data, as well as the surface tension measurements.

The outcome of our simulations for the mixture with $\chi_{TFSI} = 0.36$, which falls in the middle of the linear region w.r.t. the contact angle measurements (see Figure 1), are displayed in Figure 3. As was emphasized in Figure 1, the contact angle

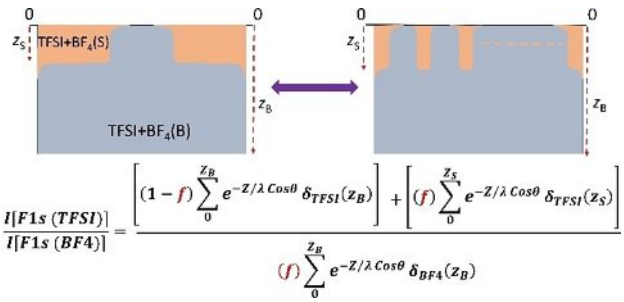

Scheme 1. Fractionally covered and TFSI enriched surface layer, together with the formula used to calculate the anion intensity ratios as a function of the photoelectron take-off angle.

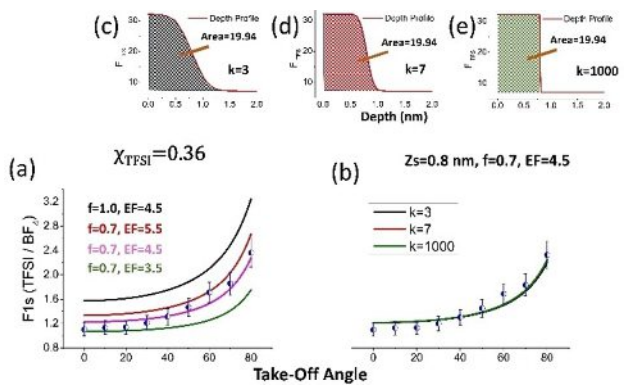

Figure 3. (a) Results of the simulations for 3 different EFs together with the raw F1s ratios determined by AR-XPS of the 0.36 TFSI mole fraction for one geometry with different EFs for the TFSI Enriched Layer. The data for a complete covered (f = 1) layer with EF = 4.5 is also included. **(b)** Similar data with 3 different geometries having the same integrated EF of 4.5 are schematically shown in **(c)**, **(d)** and **(e).**

measurement for this mixture also indicated an enrichment of the TFSI anions to a surface mole fraction of 0.70, which can also be interpreted as an apparent fractional coverage. Figure 3(a) displays our simulations using this fraction for three different EFs and the experimental data for a nominal thickness of 0.8 nm enriched layer. As can be gathered from the figure EF of 4.5 gives the best match with the AR-XPS results. Shown in the same figure is the very poor fit of the simulation data for the full coverage (f = 1). This EF of 4.5 is in agreement with the same factor estimated using the surface tension derived surface to bulk mole fraction ratio (0.70/0.30)/(0.36/0.64) = 4.1

In Figure 3(b) we show additional data obtained using three widely different distribution functions, having the same integrated total enrichment factor, indicating surprisingly the independency of the result to the shape of the distribution function (Figure 3(c, d and e)) and attenuation length (λ) used in simulations (Figure S11). Very similar results are obtained for the more dilute solutions of 0.24, where the effective surface tension was indicating it to be 0.42 in Figure 1. Our findings are compiled in Table S2 in the SI section, for all the mixtures investigated.

AR-XPS data shows a substantial TFSI enrichment at the topmost layers, especially for mixtures having mole fraction lower than 0.5. The contact angle measurements show a steeper gradual decrease in the same mole fraction regime (from 0.10 to 0.67) (Figure 1). Above this mole fraction the percent surface enrichment decreases. At the same time, the cosine of the contact angles reaches to the contact angle value of pure DEME-TFSI. The surface is always dominated by the $TFSI^-$ and $DEME^+$ molecular ions, whereas BF_4^- is depleted from the surface layer. The surface structure is more intriguing for smaller mole fractions. Although these ILs are completely miscible in the bulk,[5a] TFSI has a higher surface propensity compare to BF_4^-, which is more pronounced at lower mole fractions of TFSI (0.10–0.36) evident by the AR-XPS as well as the contact angle data.

The surface enriched layer is extracted to be ~0.8 nm from the geometrical model. Such an apparent surface layer thickness is reasonable based on the well-known surface access thickness of air/water interface and considering the molecular size of the IL ions. Therein, the surface layer has been assigned to the topmost 1–2 layers of water (~0.5 nm) at the air/water interface, where the size of one water molecule is ~0.3 nm.[21] In analogy, the topmost 1–2 layers of bulky molecular ions in IL is expected to have ~0.8 nm for the surface layer, consistent with reports on similar systems.[22] Furthermore, examining our mean-field simulation with different parameter values, we were able to demonstrate that an enriched surface layer thicker than 1 nm (Figure S9) and smaller than 0.5 nm (Figure S12(a)) are incompatible with the AR-XPS data. Moreover, fitting the data using only two angles (0° and 80°) would have resulted in a thickness of 0.2 nm (Figure S12(a)), that is unrealistic considering the size of the bulky ions. Additionally, other fitting routines, using only part of the AR-XPS data sets, or using other functions, have also been applied to further validate our simulation approach. (See Figure S12(b) for details.)

In summary, by using AR-XPS and surface tension measurements together with our signal attenuation model, we determined that the vacuum interface of the liquid IL mixtures are fractionally covered by anion enriched surface layers of ~0.8 nm thickness. Our work clearly demonstrated the surface propensity of one IL anion ($TFSI^-$) over the other one (BF_4^-) in the binary IL mixture. Hence, AR-XPS technique, utilizing the full-range of the angles, can also be used to assess the surface layering structure in liquids.

Naturally, there may be several overlooked issues and pitfalls in our mean-field approach, but we are hoping that others will take up from here on and explore with well-defined and validated liquid samples. We must also remind that, historically, the AR-XPS began on analyses of solids and thin-film surfaces, and had taken more than 3 decades to ripen and to reach its current status as a reliable and indispensable tool,[19] but only via a massive cooperation of the community, and using innumerable validated samples and cross-referencing them with other complementing techniques.

Acknowledgements

This work is supported by Grant No: 118Z902 of the Scientific and Technological Research Council of Turkey (TUBITAK).

Conflict of Interest

The authors declare no conflict of interest.

Keywords: angle-resolved XPS · attenuation model · ionic liquid mixtures · surface enrichment · surface tension

[1] a) T. Welton, *Biophys. Rev. Lett.* **2018**, *10*, 691–706; b) K. S. Egorova, E. G. Gordeev, V. P. Ananikov, *Chem. Rev.* **2017**, *117*, 7132–7189; c) M. Watanabe, M. L. Thomas, S. G. Zhang, K. Ueno, T. Yasuda, K. Dokko, *Chem. Rev.* **2017**, *117*, 7190–7239; d) S. Eftekhari *Energy Storage Mater.* **2017**, *9*, 47–69.
[2] Y.-L. Wang, B. Li, S. Sarman, F. Mocci, Z.-Y. Lu, J. Yuan, A. Laaksonen, M. D. Fayer, *Chem. Rev.* **2020**, doi:10.1021/acs.chemrev.9b00693.
[3] a) H. Niedermeyer, J. P. Hallett, I. J. Villar-Garcia, P. A. Hunt, T. Welton, *Chem. Soc. Rev.* **2012**, *41*, 7780–7802; b) G. Chatel, J. F. Pereira, V. Debbeti, H. Wang, R. D. Rogers, *Green Chem.* **2014**, *16*, 2051–2083.
[4] a) I. J. Villar-Garcia, K. R. J. Lovelock, S. Men, P.. Licence, *Chem. Sci.* **2014**, *5*, 2573–2579; b) R. Hayes, G. O. Warr, R. Atkin, *Chem. Rev.* **2015**, *115*, 6357–6426.
[5] a) M. T. Clough, C. R. Crick, J. Gräsvik, P. A. Hunt, H. Niedermeyer, T. Welton, O. P. Whitaker, *Chem. Sci.* **2015**, *6*, 1101–1116; b) R. P. Matthews, I. J. Villar-Garcia, C. C. Weber, J. Griffith, F. Cameron, J. P. Hallet, P. A. Hunt, T. Welton *Phys. Chem. Chem. Phys.* **2016**, *18*, 8608–8624; c) S. Palchowdhury, B. L. Bhargava, *J. Phys. Chem. C* **2016**, *120*, 5430–5441; d) S. Men, P. Licence, *Chem. Phys. Lett.* **2017**, 681, 40–43; e) R. Costa, I. V. Voroshylova, M. N. D. Cordeiro, C. M. Pereira, A. F. Silva, *Electrochim. Acta* **2018**, *261*, 214–220; f) E. J. Smoll, M. Tesa-Serrate, S. Purcell, L. D'Andrea, D. Bruce, J. Slattery, M. L. Costen, T. K. Minton, K. G. McKendrick, *Faraday Discuss.* **2018**, *206*, 497–522.
[6] I. J. Villar-Garcia, S. Fearn, N. L. Ismail, A. J. S. McIntosh, K. R. J. Lovelock, *Chem. Commun.* **2015**, *51*, 5367–5370.
[7] R. Atkin, G. G. Warr, *J. Phys. Chem. C* **2007**, *111*, 5162–5168.
[8] I. S. Martinez, S. Baldelli, *J. Phys. Chem. C* **2010**, *114*, 11564–11575.

[9] a) D. Wakeham, G. G. Warr, R. Atkin, *Langmuir* **2012**, *28*,13224–13231; b) D. W. Bruce, C. P. Cabry, J. N. C. Lopes, M. L. osten, M. L. D'Andrea, I. Grillo, B. C. Marshall, K. G. McKendrick, T. K. Minton, S. M. Purcell, *J. Phys. Chem. B* **2017**, *121*, 6002–6020.
[10] a) K. Nakajima, M Miyashita, M. Suzuki, K. Kimura, *J. Chem. Phys.* **2013**, *139*, No. 224701; b) K. Nakajima, S. Nakanishi, Z. Chval, M. Lísal, K. Kimura, *J. Chem. Phys.* **2016**, *145*, No. 184704; c) K. Nakajima, S. Nakanishi, M. Lísal, K. Kimura, *J. Mol. Liq.* **2017**, *230*, 542–549.
[11] I. J. Villar-Garcia, S. Fearn, G. F. De Gregorio, N. L. Ismail, F. J. V. Gschwend, A. J. S. McIntosh, K. R. J. Lovelock, *Chem. Sci.* **2014**, ***5***, 4404–4418.
[12] a) V. Lockett, R. Sedev, C. Bassell, J. Ralston, *Phys. Chem. Chem. Phys.* **2008**, *10*, 1330–1335; b) K. R. J. Lovelock, C. Kolbeck, T. Cremer, N. Paape, P. S. Schulz, P. Wasserscheid, F. Maier, H. P. Steinrück, *J. Phys. Chem. B* **2009**, *113*, 2854–2864; c) K. R. J. Lovelock, *Phys. Chem. Chem. Phys.*, **2012**, *14*, 5071–5089.
[13] a) G. Garcia, M. Atilhan, S. Aparcio, *J. Phys. Chem. C* **2015**, *119*, 28405–28416; b) K. Shimizu, B. S. J. Heller, F. Maier, H. P. Steinrück, J. N. C. Lopes, *Langmuir* **2018**, *34*, 4408–4416.
[14] *Chemical Reviews* **2017**, *117*, 10, 6633–7240.
[15] a) O. Russina, F. Lo Celso, N. V. Plechkova, A. Triola, *J. Phys. Chem. Lett.* **2017**, *8*, 1197–1204; b) T. Tyler Cosby, U. Kapoor, J. K. Shah, J. Sangoro, *J. Phys. Chem. Lett.* **2019**, 10, 6274–6280; c) Y. Zhang, Y. Khalifa, E. J. Maginn, J. T. Newberg, *J. Phys. Chem. C* **2018**, *122*, 27392–27401.
[16] a) B. S. J. Heller, C. Kolbeck, I. Niedermaier, S. Dommer, J. Schatz, P. Hunt, F. Maier, H. P. Steinrück, *ChemPhysChem* **2018**, *19*, 1733–1745; b) B. S. J. Heller, U. Paap, F. Maier, H. P. Steinrück, *J. Mol. Liq.* **2020**, *305*, 112783.
[17] P. Mack, R. G. White, J. Wolstenholme, T. Conard, *Appl. Surf. Sci.* **2006**, *252*, 8270–8276.
[18] M. Tariq, M. G. Freiire, B. Saramago, J. A. P. Countinho, J. N. C. Lopes, L. N. P. Rebelo, *Chem. Soc. Rev.* **2012**, *41*, 829–868.
[19] P. B. Petersen, R. J. Saykally, *Annu. Rev. Phys. Chem.* **2006**, *57*, 333–364.
[20] C. J. Powell, A. Jablonski, NIST Electron Inelastic-Mean-Free-Path Database - Version 1.2, National Institute of Standards and Technology, Gaithersburg, MD, **2010**.
[21] a) P. Jungwirth, D. J. Tobias, *J. Phys. Chem. B* **2002**, *106*, 6361–6373; b) Y. Fan, X. Chen, L. Yang, P. S. Cremer, Y. Q. Gao, *J. Phys. Chem. B* **2009**, *113*, 11672–11679.
[22] M. Mezger, H. Schröder, H. Reichert, S. Schramm, J. S. Okasinski, S. Schöder, V. Honkimäki, M. Deutsch, B. M. Ocko, J. Ralston, M. Rohwerder, M. Stratmann, H. Dosch, *Science* **2008**, *322*, 424–428.

Manuscript received: September 1, 2020
Revised manuscript received: September 18, 2020
Accepted manuscript online: September 21, 2020
Version of record online: October 14, 2020